Comparison of terahertz waveforms measured by electro-optic and photoconductive sampling

Sang-Gyu Park,[a] M. R. Melloch, and A. M. Weiner
School of Electrical Engineering, Purdue University, 1285 EE Building, West Lafayette, Indiana 47907-1285

(Received 16 July 1998; accepted for publication 28 September 1998)

Terahertz waveforms measured by free-space electro-optic sampling and a photoconductive dipole antenna were carefully compared. We show that the difference between the waveforms could be explained quantitatively in terms of carrier lifetime and frequency dependent response of the photoconductive receiver antenna. © *1998 American Institute of Physics.* [S0003-6951(98)00748-7]

Since its invention in the 1980's, photoconductive (PC) sampling has been widely used to measure the terahertz (THz) electric field coherently generated by femtosecond lasers.[1,2] Its high signal to noise ratio has enabled many THz applications including spectroscopy,[3,4] imaging,[5] and ranging.[6] But its speed is limited by the resonant characteristic of the antenna structure and the finite lifetime of the photogenerated carriers in the detector. Recently free-space electro-optic sampling (FS-EOS) of THz radiation was demonstrated to be an alternative to PC-sampling.[7] Due to its high bandwidth and ease of implementation, it is becoming increasingly popular. Despite the wide use of PC-sampling and FS-EOS, the waveforms measured by the two methods have not been compared closely. The comparison has mainly been limited to the speed and the signal to noise ratio.[8,9] In this letter, we quantitatively compare the waveforms measured by these two methods and demonstrate a simple modeling procedure that predicts the PC-sampling waveform directly from the measured FS-EOS waveform.

FS-EOS detects the polarization change of the probe beam induced by THz electric field through the electro-optic (E-O) effect in the sensor crystal. Because the E-O effect is almost instantaneous on the THz time scale, especially in compound semiconductors, FS-EOS gives a signal directly proportional to the THz electric field. Although there are several effects which could distort measured waveforms, including group velocity mismatch (GVM) between copropagating optical probe and THz beams, phonon-polariton coupling and finite probe pulse width, waveform distortion from these effects is minimal for the pulse width, crystal thickness, and THz bandwidth used in our experiments.

On the other hand, measurements with a PC-antenna receiver generate waveforms which depend not only on the actual THz electric field $e(t)$ incident at the receiver, but also on the frequency dependent antenna response $H(\omega)$ and the carrier lifetime τ_R and momentum relaxation time τ_C. The collected charge Q as a function of delay τ of the gating pulse is given by

$$Q(\tau)=\int dt\,\nu(t)g(t-\tau), \tag{1}$$

where the induced bias voltage across the photoconductive gap $\nu(t)$ is

$$\nu(t)\sim\int d\omega H(\omega)E(\omega)\exp(i\omega t), \tag{2}$$

and the time dependent conductance $g(t)$ is

$$g(t)=\int^{t} dt' I(t')\{1-e^{-(t-t')/\tau_C}\}e^{-(t-t')/\tau_R}. \tag{3}$$

Here, $I(t)$ is the temporal intensity profile of the gating pulse and $E(\omega)$ is the Fourier transform of $e(t)$. The finite photocurrent rise time and the current recovery time are represented by τ_C and τ_R, respectively.[10] The response function $H(\omega)$ represents the frequency dependent ratio of voltage induced at the sampling gap to incident electric field $E(\omega)$, where $E(\omega)$ is assumed to approximate a plane wave at the receiver. $H(\omega)$ depends on the coupling of the incident wave onto the antenna as well as the impedance matching conditions between the antenna and the transmission line in which it is embedded; both of these factors may be frequency dependent. As reported in the following, for our experiments on a short dipole antenna without substrate lens, we find a flat frequency response $[H(\omega)=1]$ gives a good fit to our data; i.e., $\nu(t)$ is directly proportional to the incoming electric field profile. This is in marked contrast to the well-known $j\omega$ frequency dependence of a short dipole transmitting antenna. The flat frequency response can be explained as follows. Because the overall length of the dipole antenna is much shorter than the shortest wavelength of the incoming electric field, the electric field $E(\omega)$ (for any given ω) is spatially uniform across the antenna times a frequency independent constant. Therefore, the induced open circuit voltage, $V_{oc}(\omega)$, is just $E(\omega)$ multiplied by the length of the antenna.[11] The actual voltage across the gap, V_g, when there is a transmission line feed connected to the antenna, can be calculated from the following voltage divider expression $V_g=V_{oc}Z_o/(Z_0+Z_A)$, where Z_0 and Z_A are the impedances of the transmission line and antenna, respectively. The radiation impedance of our short dipole is small in the frequency region of interest between tens of GHz and 2 THz. (At very low frequency the antenna reactance becomes large and this leads to a zero dc response.) When Z_A is small compared to Z_o, V_g can be approximated by V_{oc}. Therefore, if the measurement is limited to the THz range where the wavelength

[a]Electronic mail: sanggyu@ecn.purdue.edu

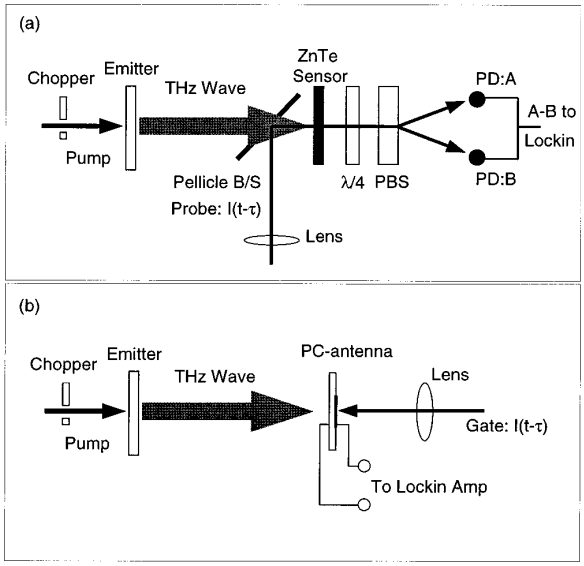

FIG. 1. Experimental setup: (a) free-space electro-optic sampling; (b) photoconductive sampling. (B/S: beam splitter, PD: photodiode, PBS: polarization beam splitter).

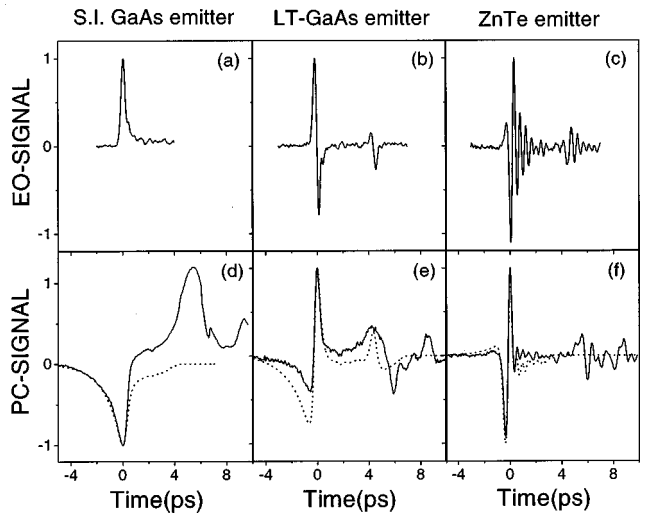

FIG. 2. Measured and calculated THz waveforms using EO and PC sampling: (a)–(c): EO-sampled waveforms; (d)–(f): PC-sampled waveforms (measurement: solid line, calculation: dotted line). The PC receiver was a short dipole with no substrate lens.

is much longer than the antenna length, both the open circuit voltage and the voltage divider effect are nearly frequency independent. On the other hand, we find that for a short dipole receiver with a substrate lens, $H(\omega) \sim j\omega$ gives a good fit to the data in the specific optical system of our experiments.

Figure 1 shows the experimental setups for our comparison of FS-EOS and PC sampling. In each case, the receiver (either FS-EOS or PC) was placed at the same position relative to the THz source. Our approach is to use the waveforms measured by FS-EOS as the real electric field waveform $e(t)$ in Eqs. (1)–(3) in order to predict the expected PC-sampled waveforms. Since the PC-sampled waveforms and the EO-sampled waveforms are measured at the same position, we do not need to know the transfer function of the THz pulse from emitter to detector, which would be the same for both waveforms. This is in contrast to the situation where the measured THz waveforms are modeled based on the knowledge of the field at the emitter. We performed our comparison for three different sources of THz radiation, namely, two different biased large aperture GaAs emitters and an unbiased ZnTe large aperture emitter. The three emitters generated very distinct waveforms, which helped to confirm the validity of our theory. The biased emitters were fabricated by deposition of 3 mm spaced parallel electrodes either on semi-insulating GaAs (SI-GaAs) or low temperature grown GaAs (LT-GaAs).[12] The LT-GaAs layer was grown at 280 °C and annealed at 575 °C for 30 s. We used a thick (2.8 μm) LT-GaAs epitaxial layer in order to minimize the partial transmission of the excitation pulse into the SI-GaAs substrate. The unbiased ZnTe emitter was $\langle 110 \rangle$ oriented and 1 mm thick. In the biased emitters, THz radiation is generated due to current surges and the far field radiation is given by the time derivative of the photogenerated current. In the unbiased ZnTe emitters, optical rectification is responsible for the THz generation.[13] For the FS-EOS receiver, we used a 150-μm-thick ZnTe crystal with balanced detection. We used a relatively thin sensor crystal to minimize the waveform distortion by phonon-polariton coupling and GVM. For the PC-antenna receiver, we used a 50-μm-long dipole antenna with 5 μm gap[14] embedded in a 50 μm spaced coplanar transmission line and fabricated on the LT-GaAs. The LT-GaAs was grown at the same time as the emitter material but annealed at slightly higher temperature (600 °C). A mode-locked Ti: sapphire laser with ~100 fs pulse width was used to provide pump and time delayed probe pulses. The pump power was 800 mW for all cases and the probe power was 2 mW for FS-EOS and 20 mW for PC-antenna detection. The pump beam was collimated with a diameter of 1 mm. The emitters and detection systems were separated by ~15 cm with no focusing for the THz beam or pump beam, which were well into the far-field regime.

Figures 2(a)–2(c) show the measured THz waveforms from FS-EOS. We can clearly see the difference between the waveforms from different emitters. From the SI-GaAs emitter, we obtained an almost unipolar waveform, which is in sharp contrast to the bipolar waveform obtained from the LT-GaAs emitter. This was expected from the lifetime of photogenerated electrons in these materials. Because of very long carrier lifetime, SI-GaAs has step-like current profile, which gives unipolar waveforms. LT-GaAs has a very short carrier lifetime, therefore, both rising and falling edges of the current can generate a strong THz field, resulting in bipolar waveforms. The waveform from the ZnTe emitters has a strong ringing associated with the main oscillation. This ringing seems to be from the emitter, not from the sensor. When we changed to a 1-mm-thick sensor, the ringing remained almost the same, while when we changed to a 150 μm emitter with the default 150 μm sensor, the ringing almost disappeared. Figures 2(d)–2(f) show the corresponding waveforms measured by PC sampling (solid lines). Note that no substrate lens was used for these PC-sampling measurements. In each case, the shapes of the PC and the corresponding FS-EOS waveforms are markedly different. Figures 2(d)–2(f) also show the predicted PC-sampling waveforms (dotted lines), which were calculated based on Eqs. (1)–(3) using the FS-EOS data for the incident THz

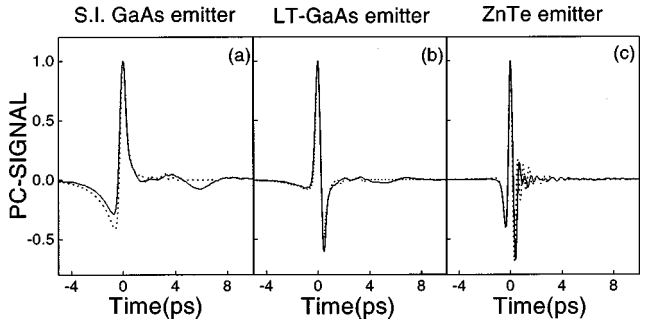

FIG. 3. THz waveforms from PC sampling with silicon lens. The reflection feature from the EO sampled waveform was numerically eliminated before used in the calculation. (measurement: solid line, calculation: dotted line).

field $e(t)$. As fitting parameters we used a carrier lifetime $\tau_R = 1.3$ ps (in agreement with optical pump/probe time resolved reflection measurements and sliding contact photoconductive sampling measurements), and a momentum relaxation time $\tau_C = 0.18$ ps. We use a flat antenna response function $H(\omega) = 1$, for which the derived and measured waveforms match fairly well. We used the same fitting parameters to calculate waveforms corresponding to each of the three THz emitters. In the data the features 5–6 ps after the main peaks are from reflections in the FS-EOS and PC detectors. (This was not accounted for in the simulation.) The initial dip before the main features of the PC waveforms is associated with the lifetime of the photogenerated carriers, and is most clearly observed for the unipolar waveform from the SI-GaAs emitter. For the bipolar waveforms, this effect is less pronounced, because the positive and negative portions of the waveform partially cancel out in the convolution in Eqs. (1)–(3). The agreement between simulated and measured waveforms for all three emitters validates our approach for modeling the PC-receiver response.

For practical THz systems, the PC antenna is usually used together with a substrate lens, in order to increase the coupling of the THz energy to the antenna.[14] The effect of such lenses on the waveforms has been discussed by several authors.[5,14,15] We have repeated our PC-sampling experiments with a hyperhemispherical silicon lens attached to the PC antenna. The diameter and the tip to bottom distance of the silicon lens were 10 and 6.5 mm, respectively, and the thickness of the GaAs PC receiver chip was 0.63 mm. This design is similar to that used in Ref. 14. The results of the measurement are shown in Fig. 3. We can see distinct differences between the waveforms in Fig. 3 and the corresponding PC waveforms in Fig. 2. Besides the waveform changes, the amplitude of the THz signal was enhanced by more than a factor of 10 by using the silicon lens. Also shown in Fig. 3 are calculated PC waveforms derived from the FS-EOS data, with the same τ_R and τ_C as before (dotted lines). In this case we use an antenna response function $H(\omega) = j\omega$, which gives excellent agreement with the data waveforms. The $j\omega$ factor leads to a derivative-like behavior in the time domain. Our results may be understood as follows. The Fourier spectrum analysis of the EO waveform (not shown) indicates that the majority of the THz power from our emitters is emitted between dc and 2 THz. In our back to back configuration, the THz beam at the receiver chip is larger than the silicon lens aperture for all the frequencies below 2 THz. For example, we calculate beam diameters (at the e^{-1} points of the field) of 29 and 15 mm for 1 and 2 THz, respectively. Therefore, the aperture is defined by the lens diameter and is approximately frequency independent, resulting in a focused THz spot size which is inversely proportional to frequency. Since the spot sizes are also larger than the dipole itself, this gives the observed $j\omega$ frequency factor. It is interesting to note that the condition that the beam size is larger than the silicon lens is approximately equivalent to the far field criterion of the emitter/detector system including the silicon lens aperture. It is also important to note that observation of this effect depends on the specific THz optical system and frequency range. Grischkowsky *et al.* observed a similar time derivative behavior for a different THz optical system.[14] Silicon lens and optical system designs which do not have a frequency dependent spot size have also been proposed and demonstrated.[5]

In conclusion, we directly compared the THz radiation waveforms measured from FS-EOS and PC-sampling receivers. Although we observed significant differences between the two types of waveforms, we demonstrated that the waveforms measured by the PC antenna could be derived from the FS-EOS waveforms in conjunction with the carrier lifetime of the PC-antenna material. For a PC THz receiver consisting of a short dipole without substrate lens, we found that the receiver antenna response was approximately flat over the THz frequency range of interest. For the same receiver with substrate lens, we found a $j\omega$ receiver antenna response which we explained based on the specific optical system in use. Our results help to elucidate the role of the frequency-dependent antenna response in PC sampling THz receivers.

The authors acknowledge helpful discussions with Dr. X.-C. Zhang. This work was supported by National Science Foundation. M.R.M. acknowledges support by AFOSR Grant No. F49620-96-1-0234A.

[1] D. H. Auston, K. P. Cheung, and P. R. Smith, Appl. Phys. Lett. **45**, 284 (1984).
[2] P. R. Smith, D. H. Auston, and M. C. Nuss, IEEE J. Quantum Electron. **24**, 255 (1988).
[3] D. Grischkowsky, S. Keiding, M. van Exter, and Ch. Fattinger, J. Opt. Soc. Am. B **7**, 2006 (1990).
[4] I. Brener, D. Dykaar, A. Frommer, L. N. Pfeiffer, J. Lopata, J. Wynn, K. West, and M. C. Nuss, Opt. Lett. **21**, 1924 (1996).
[5] D. M. Mittleman, R. H. Jacobsen, and M. C. Nuss, IEEE J. Sel. Top. Quantum Electron. **2**, 679 (1996).
[6] R. A. Cheville and D. Grischkowsky, Appl. Phys. Lett. **67**, 1960 (1995).
[7] Q. Wu and X.-C. Zhang, IEEE J. Sel. Top. Quantum Electron. **2**, 693 (1996).
[8] Q. Wu, F. G. Sun, P. Campbell, and X.-C. Zhang, Appl. Phys. Lett. **68**, 3224 (1996).
[9] Y. Cai, I. Brener, J. Lopata, J. Wynn, L. Pfeiffer, J. B. Stark, Q. Wu, X.-C. Zhang, and J. Federici, Appl. Phys. Lett. **73**, 444 (1998).
[10] D. Grischkowsky and N. Katzenellenbogen, in *OSA Proceedings on Psec. Electronics and Optoelectronics*, edited by T. C. L. G. Sollner and J. Shah (Optical Society of America, Washington, DC, 1991), p. 9.
[11] G. D. Monteath, *Applications of the Electromagnetic Reciprocity Principle* (Pergamon, New York, 1973).
[12] M. R. Melloch, D. D. Nolte, J. C. P. Chang, D. B. Janes, and E. S. Harmon, Crit. Rev. Solid State Mater. Sci. **21**, 189 (1996).
[13] X.-C. Zhang, Y. Jin, and X. F. Ma, Appl. Phys. Lett. **61**, 2764 (1992).
[14] M. van Exter, Ch. Fattinger, and D. Grischkowsky, Appl. Phys. Lett. **55**, 337 (1989).
[15] P. U. Jepsen, R. H. Jacobsen, and S. R. Keiding, J. Opt. Soc. Am. B **13**, 2424 (1996).